

Small Molecules That Recapitulate the Early Steps of Urodele Amphibian Limb Regeneration and Confer Multipotency

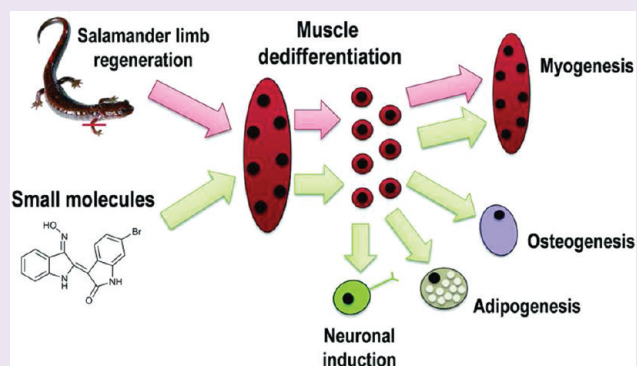
Woong-Hee Kim,^{†,‡} Da-Woon Jung,^{†,‡} Jinmi Kim,[†] Sin-Hyeog Im,[‡] Seung Yong Hwang,[§] and Darren R. Williams^{*,†}

[†]New Drug Targets Laboratory and [‡]Immune Regulation and Tolerance Laboratory, School of Life Sciences, Gwangju Institute of Science and Technology, 1 Oryong-Dong, Buk-Gu, Gwangju 500-712, Republic of Korea

[§]Department of Biochemistry, Hanyang University and GenoCheck Co., Ltd., Sa-Dong, Sangrok-Gu, Ansan, Gyeonggi-Do, 426-791, Republic of Korea

S Supporting Information

ABSTRACT: In urodele amphibians, an early step in limb regeneration is skeletal muscle fiber dedifferentiation into a cellulate that proliferates to contribute new limb tissue. However, mammalian muscle cannot dedifferentiate after injury. We have developed a novel, small-molecule-based method to induce dedifferentiation in mammalian skeletal muscle. Muscle cellularization was induced by the small molecule myoseverin. Candidate small molecules were tested for the induction of proliferation in the cellulate. We observed that treatment with the small molecules BIO (glycogen synthase-3 kinase inhibitor), lysophosphatidic acid (pleiotropic activator of G-protein-coupled receptors), SB203580 (p38 MAP kinase inhibitor), or SQ22536 (adenylyl cyclase inhibitor) induced proliferation. Moreover, these proliferating cells were multipotent, as confirmed by the chemical induction of mesodermal-derived cell lineages. Microarray analysis showed that the multipotent, BIO-treated cellulate possessed a markedly different gene expression pattern than lineage-restricted C2C12 myoblasts, especially for genes related to signal transduction and differentiation. Sequential small molecule treatment of the muscle cellulate with BIO, SB203580, or SQ22536 and the aurora B kinase inhibitor, reversine, induced the formation of cells with neurogenic potential (ectodermal lineage), indicating the acquirement of pluripotency. This is the first demonstration of a small molecule method that induces mammalian muscle to undergo dedifferentiation and redifferentiation into alternate cell lineages. This method induces dedifferentiation in a simple, stepwise approach and has therapeutic potential to enhance tissue regeneration in mammals.



Dedifferentiation is the acquirement of a more “stem-cell-like” or multipotent state in differentiated cells, allowing subsequent differentiation into alternative tissue types.¹ Phenotype-based screening of small molecule libraries has been employed to discover new regulators of cellular development.² The use of small molecules to manipulate cellular processes has a number of advantages compared to genetic approaches.³ Small molecules also have the potential to modulate multiple, specific targets within a cell, although off-target events affecting proteins of similar conformation may be problematic.

Urodele amphibians possess a remarkable capacity for dedifferentiation and tissue regeneration.⁴ For example, an entire limb can be regenerated after amputation. This phenomenon has fascinated scientists for generations, because understanding the molecular mechanisms dictating the regeneration process should facilitate approaches to enhance tissue regeneration in humans.

An early event during urodele amphibian limb regeneration is the dedifferentiation of skeletal muscle fibers proximal to the amputation site.⁵ The fibers undergo cellularization, forming proliferating mononuclear cells that contribute to a mesenchymal

growth zone (the blastema) that will reform the lost limb.⁵ However, the potential to regenerate tissue decreases in higher vertebrates.⁶ For example, mammalian skeletal muscle cannot dedifferentiate in response to injury.^{4,6}

Different approaches have been used to induce mammalian skeletal muscle dedifferentiation. The expression of viral oncogenes in mouse myotubes induces cellularization and proliferation, followed cell cycle arrest or apoptosis.⁷ However, a subset of these dedifferentiated cells are multipotent and redifferentiate into cell types from alternate mesenchymal lineages.⁷ Expression of the homeobox-containing transcriptional repressor, *msx1*, can also induce myotube dedifferentiation and transdifferentiation.⁸ However, these approaches rely on the integration of genetic elements into the muscle nuclei, which restricts their potential as a therapy to enhance tissue regeneration.

Received: August 4, 2011

Accepted: January 23, 2012

Published: January 23, 2012

Recent approaches to induce myotube dedifferentiation have employed siRNA-based strategies. Recent work from our own laboratory showed that dedifferentiation could be achieved by knockdown of the cyclin-dependent kinase inhibitor p21 (CDKN 1A, CIP1) in combination with small molecules that induce cellularization and multipotency.⁹ Knockdown of both cyclin-dependent kinase inhibitor 2A (CDKN2A, ARF) and retinoblastoma protein (RB1, OSRC) also causes cell cycle reentry in differentiated myocyte nuclei, loss of differentiation properties, and upregulation of cytokinetic machinery.¹⁰ However, siRNA-based approaches can induce nonspecific cytotoxicity, and their development as a potential therapy is more problematic compared to small molecules.^{11,12}

Herein, we present a small molecule method that can induce mammalian muscle dedifferentiation. Previous data have shown that optimal myotube cellularization is achieved using myoseverin 10.¹³ However, the cellularized myotubes did not proliferate.¹⁴ We tested four candidate small molecules for the induction of proliferation in cellularized C2C12 murine skeletal muscle: lysophosphatidic acid (LPA; pleiotropic activator of G-protein-coupled receptors) 7, SQ22536 (adenylyl cyclase inhibitor) 14, SB203580 (p38 mitogen-activated protein (MAP) kinase inhibitor) 13, and BIO (glycogen synthase-3 kinase inhibitor) 2. LPA and SQ22536 were selected as potential inducers of cellulate proliferation because they can reduce p21 expression in senescent human fibroblasts.¹⁵ p21 is a “gate-keeper” of skeletal muscle terminal differentiation.¹⁶ SB203580 was selected because p38 MAP kinase inhibition blocks muscle differentiation and reduces p21 stability.^{17,18} BIO was selected because it can induce dedifferentiation in terminally differentiated mammalian cardiomyocytes.¹⁹ In addition, we provide evidence that our small molecule strategy can induce pluripotency in dedifferentiated muscle, as shown by redifferentiation into cell types representing the mesenchymal and ectodermal lineages.

RESULTS AND DISCUSSION

Chemical approaches to modulate cell fate is an important area of chemical biology research.² The demonstration of mammalian muscle dedifferentiation using small molecules should be of interest to the chemical biology community.

BIO, SB203580, SQ22536, and LPA Induce DNA Synthesis and Cell Cycle Reentry. Small molecules used in this study are shown in Figure 1. A schematic of the protocol to measure proliferation in the muscle cellulate is shown in Figure 2A. Concentrations of compounds were based on previous reports of their activity.^{15,17,19} Cellulate treated with 2.5 μ M BIO, 10 μ M SB203580, 300 μ M SQ22536, or 30 μ M LPA for 48 h increased BrdU incorporation, indicating increased DNA synthesis (Figure 2B). BrdU incorporation was relatively smaller in the cellulate treated with SQ22536. For negative controls, two compounds were selected: MPc11 (inhibitor of the F1F0 mitochondrial ATP synthase²⁰) 9 and magnesium lithospermate B (MLB; naturally occurring antioxidant²¹) 8. Treatment with 50 μ M MLB or 5 μ M MPc11 for 48 h did not increase proliferation (Figure 2B). None of the compounds induced cytotoxicity (Figure 2C). Interestingly, the canonical myoblast growth factors hepatocyte growth factor and basic fibroblast growth factor²² did not induce proliferation (Supplementary Figure 1).

7-AAD staining of cellulate treated with BIO was not possible, because BIO caused cell staining. The MTT assay was used to show that treatment with 2.5 μ M BIO for 48 h was not cytotoxic

(Figure 2D). Nuclear staining showed that BIO, SB203580, SQ22536, or LPA increased the percentage of cells in the G₂-M phase of the cell cycle, indicating cell cycle reentry (Figure 2E).

BIO, SB203580, SQ22536, or LPA Modulates CDKN Expression. Cyclin-dependent kinase inhibitors (CDKN) are implicated in maintaining skeletal muscle differentiation, including p21 (CIP1/CDKN1A), p27 (CDKN1B/KIP1), and p57 (CDKN1C/KIP2).^{16,23} Treatment with BIO or SB203580 decreased p57 expression (Figure 3A). However, treatment did not markedly affect p27 expression (Figure 3A). In contrast, compound treatment reduced p21 expression (Figure 3A).

BIO, SB203580, and LPA Induce Dedifferentiation in Cellularized Myotubes. α -Bungarotoxin is a ligand for the acetylcholine receptor expressed in differentiated skeletal muscle. Treatment with BIO, SB203580, or LPA reduced FITC-conjugated α -bungarotoxin labeling, indicating dedifferentiation (Figure 3B). Treatment with SQ22536, MLB, or MPc11 did not reduce α -bungarotoxin labeling (Figure 3B). Fluorescent plate reader assay confirmed that BIO, SB203580, or LPA reduced α -bungarotoxin labeling (Figure 3C).

BIO, SB203580, SQ22536, or LPA Does Not Affect Myogenic Potential. The ability of the muscle cellulate to form muscle (myogenic potential) was assessed using the fusion index.⁹ BIO, SB203580, SQ22536, or LPA did not affect the fusion index (Figure 3D). In contrast, treatment with reversine 12 decreased the fusion index.

BIO, SB203580, SQ22536, or LPA Induces Adipogenic Conversion. Treatment of the C2C12 muscle cellulate with BIO, LPA, SB203580, or SQ22536, followed by culture with adipogenic factors, induced lipid accumulation, indicating adipogenic conversion (Figure 4Ai). Treatment with MLB or MPc11 and adipogenic factors did not induce lipid accumulation. Our previous study demonstrated that adipogenic conversion using p21 knockdown depended on reversine treatment.⁹ However, treatment of the C2C12 muscle cellulate with BIO, LPA, SB203580, or SQ22536, followed by adipogenic factors, induced lipid accumulation, without reversine treatment (Figure 4Aii). Insulin-stimulated uptake of glucose is another characteristic of adipocytes.²⁴ Treatment with BIO, LPA, SB203580, or SQ22536 for 48 h, followed by culture in a cocktail of adipogenic factors, induced insulin-stimulated glucose uptake (Supplementary Figure 2). For comparison, treatment with reversine and adipogenic factors, after treatment with BIO, LPA, SB203580, or SQ22536, also induced lipid accumulation and insulin-stimulated glucose uptake (Supplementary Figure 3A,B). Insulin-mediated prevention of free fatty acid release after epinephrine stimulation is an adipocyte characteristic.²⁵ Myotube-derived mononuclear cells treated with BIO, plus adipogenic factors, retained fatty acid content after epinephrine stimulation in the presence of insulin (Figure 4Aiii). The degree of fatty acid retention by adipocytes, compared to muscle cellulates, has been described in our previous study.⁹

BIO, SB203580, SQ22536, or LPA Induce Osteogenic Conversion. In higher vertebrates, endochondral ossification is the process by which the majority of bones develop.²⁶ Calcification occurs at nucleation sites in the lacunae of mineralizing cartilage.²⁷ Alizarin Red is a stain for mineralization that is used for stem cell evaluation and osteogenic compound screening.²⁸ Treatment with BIO, LPA, SB203580, or SQ22536, followed by culture with osteogenic factors, induced mineralization (Figure 4Bi). Mineralization was observed to occur as patches in the cell population. Treatment with MLB or MPc11 and osteogenic factors did not induce mineralization. Treatment with BIO or SB203580 induced greater

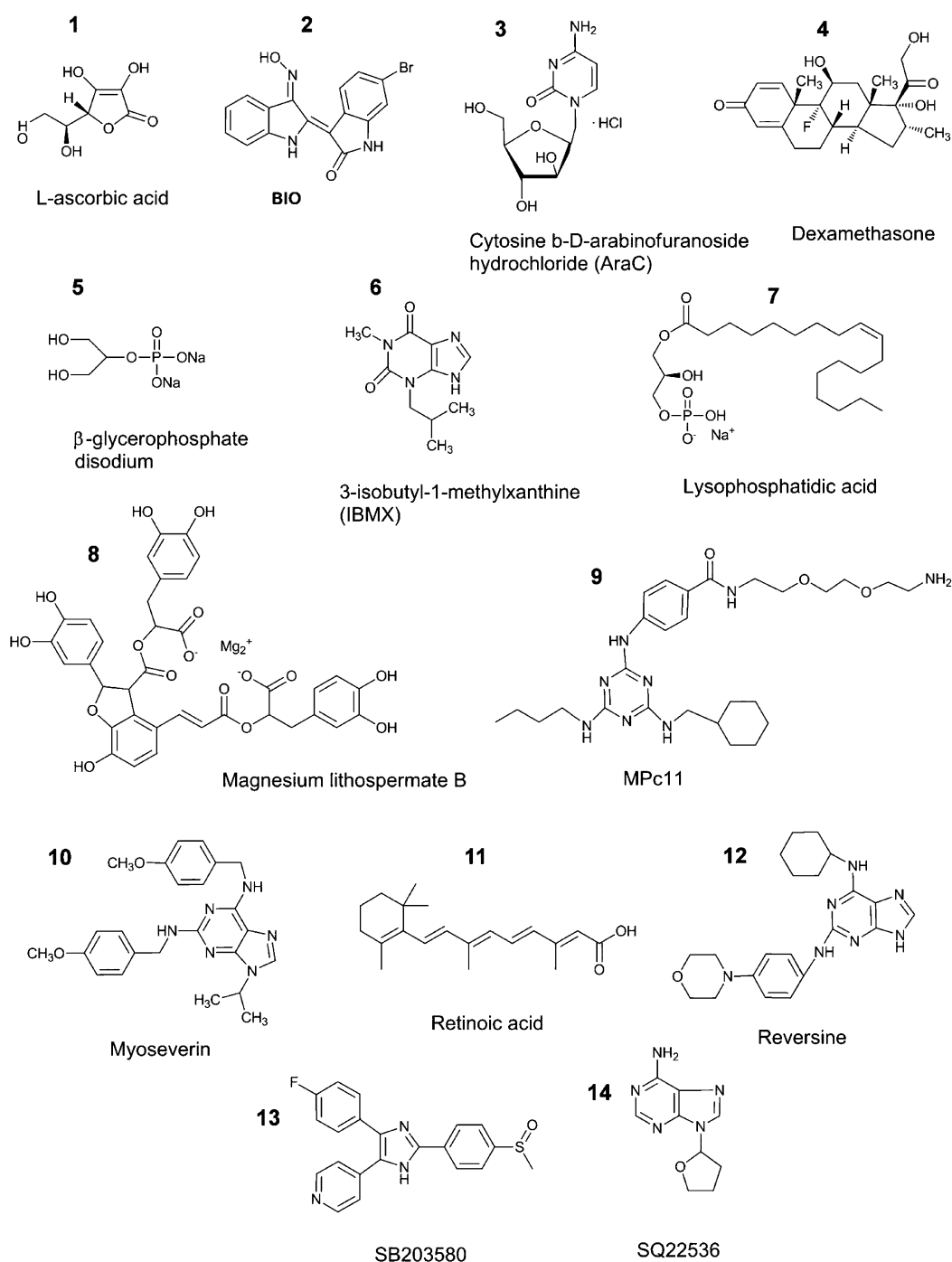


Figure 1. Structures of the small molecules used to promote skeletal muscle dedifferentiation and differentiation into alternate cell types (in alphabetical order).

mineralization after culture in osteogenic factors, compared to LPA or SQ22536 (Figure 4Bii). Treatment with BIO, LPA, SB203580, or SQ22536, plus reversine and osteogenic factors, increased the overall levels of mineralization (Supplementary Figure 3C). Treatment with BIO, LPA, SB203580, or SQ22536, plus osteogenic factors also induced alkaline phosphatase activity, indicative of osteogenic conversion (Figure 4Biii). The induction of alkaline phosphatase activity was higher in the BIO and SB203580 treated groups. Treatment with BIO, LPA, SB203580, or SQ22536, plus reversine and osteogenic factors, increased the overall levels of alkaline phosphatase activity (Supplementary Figure 3D). We also found that the

treated cellulate retained multipotent potential. BIO-treated cellulate was capable of lipid accumulation or mineralization after two culture passages over a 7 day period (Supplementary Figure 4).

BIO, SB203580, and SQ22536 Induce Neurogenic Properties. The development of neurogenic properties after compound treatment was monitored by RT-PCR analysis of Hes-6 expression (a transcription factor that promotes neuronal differentiation²⁹). Treatment with BIO, SB203580, or SQ22536, followed by culture with reversine and neurogenic factors, up-regulated Hes-6 expression (Figure 5A). Up-regulated Hes-6 expression induced morphological changes

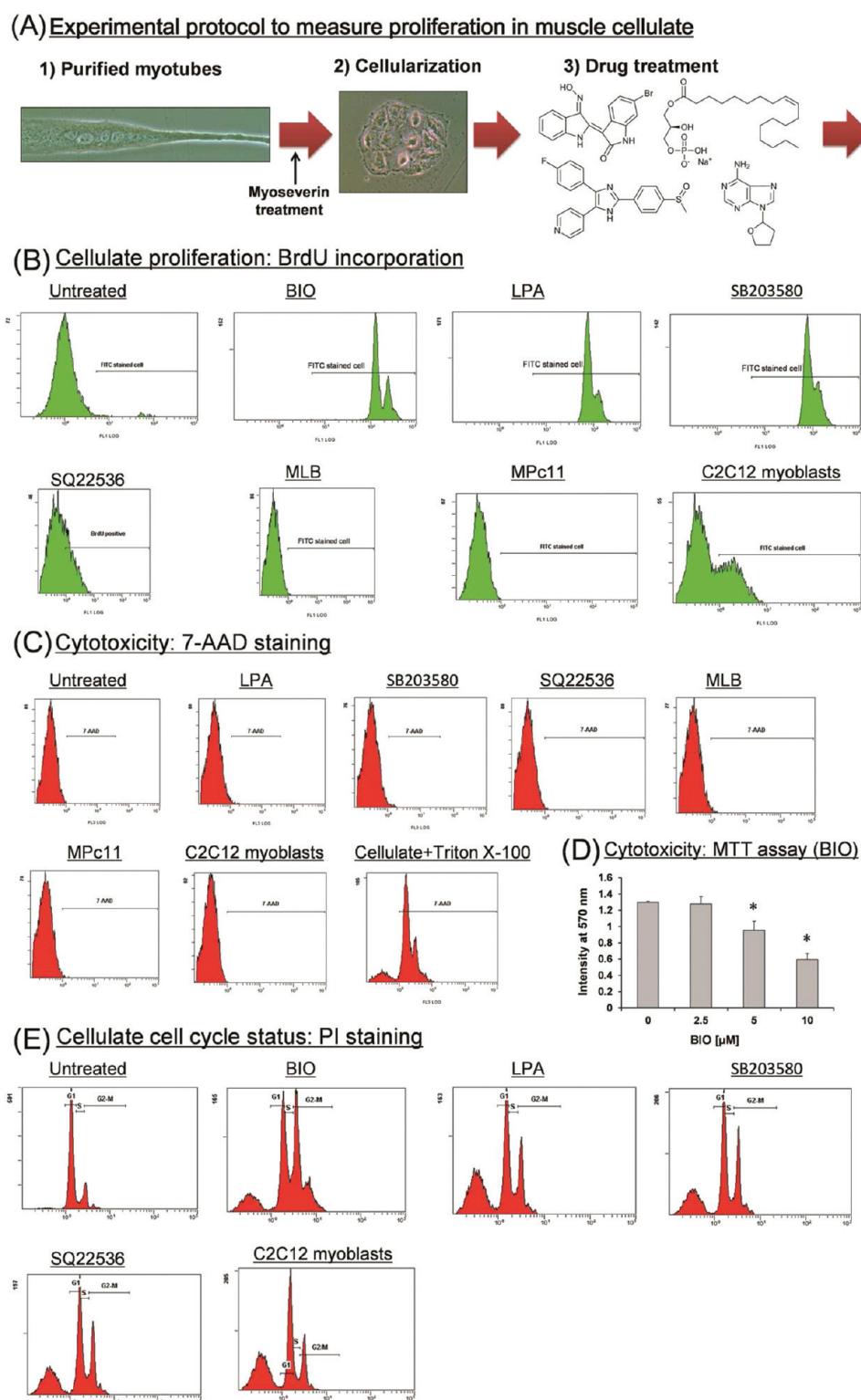


Figure 2. Analysis of cellulate proliferation. (A) Schematic of the experimental protocol used to measure cell proliferation in C2C12 differentiated mouse myotubes. (B) Treatment of the C2C12 muscle cellulate with 2.5 μ M BIO, 10 μ M SB203580, 300 μ M SQ22536, or 30 μ M LPA for 48 h induced DNA synthesis, as shown by increased FITC-BrdU signal. Treatment of the C2C12 muscle cellulate with 50 μ M MLB or 5 μ M MPc11 for 48 h did not increase DNA synthesis. C2C12 muscle precursor cells (myoblasts) were used as a positive control. (C) Treatment of the C2C12 muscle cellulate with 10 μ M SB203580, 300 μ M SQ22536, 30 μ M LPA, 50 μ M MLB, or 5 μ M MPc11 for 48 h did not induce cytotoxicity, as shown by an absence of 7-AAD staining. Treatment with 0.1% Triton X-100 in the staining solution was used as a positive control for cytotoxicity. (D) MTT assay showed that treatment of the C2C12 muscle cellulate with 2.5 μ M BIO for 48 h did not induce cytotoxicity. However, treatment with 5 or 10 μ M BIO did induce cytotoxicity. (E) Flow cytometry analysis of propidium iodide (PI) stained cellularized C2C12 myotubes showed that treatment with 2.5 μ M BIO, 10 μ M SB203580, 300 μ M SQ22536, or 30 μ M LPA for 48 h induced cell cycle reentry, as indicated by an increase in the proportion of cells in the G₂-M phase of the cell cycle. C2C12 myoblasts were used as a positive control.

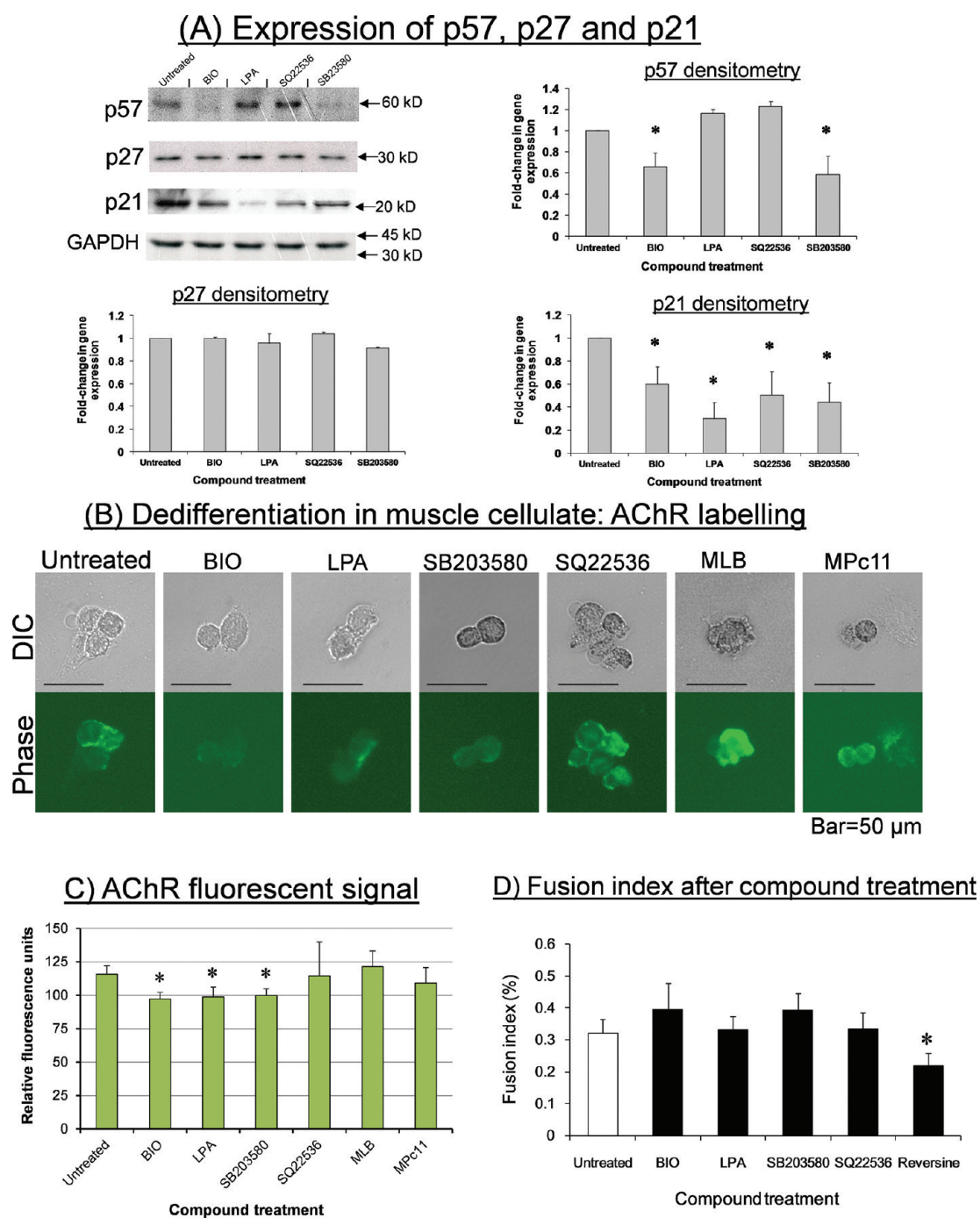


Figure 3. Analysis of cellulate dedifferentiation. (A) (i) Western blot analysis showed that treatment of the C2C12 muscle cellulate with 2.5 μM BIO or 10 μM SB203580 for 48 h reduced the expression of p57. Treatment of the C2C12 muscle cellulate with 300 μM SQ22536 or 30 μM LPA did not reduce p57 expression. However, treatment of the C2C12 muscle cellulate with BIO, SB203580, SQ22536, or LPA did not affect p27 expression. In contrast, treatment of the C2C12 muscle cellulate with BIO, SB203580, SQ22536, or LPA reduced p21 expression. GAPDH expression was used as a loading control. Densitometry analysis shows average change in band intensity for three Western blots (error = SD; * = $P < 0.05$ for reduced expression compared to untreated cellulate). (B) Treatment of the C2C12 muscle cellulate with 2.5 μM BIO, 10 μM SB203580, or 30 μM LPA for 48 h enhanced dedifferentiation, as shown by reduced expression of the differentiated muscle-specific acetylcholine receptor (detected with FITC-conjugated α -bungarotoxin). Treatment with 300 μM SQ22536, 50 μM MLB, or 5 μM MPc11 for 48 h did not appear to reduce acetylcholine receptor expression. (C) Fluorescent microplate reader assay for FITC-conjugated α -bungarotoxin labeling confirmed that treatment of the C2C12 muscle cellulate with BIO, SB203580, or LPA enhanced dedifferentiation, as shown by reduced fluorescent signal (error = SD; * = $P < 0.05$ compared to untreated cellulate). (D) Treatment of C2C12 muscle cellulate with 2.5 μM BIO, 10 μM SB203580, 300 μM SQ22536, or 30 μM LPA for 48 h did not affect the fusion index (i.e., the number of cell nuclei incorporated into multinucleate myotube syncytia) after 5 d culture in differentiation media. In contrast, treatment with 1 μM reversine for 48 h caused a decrease in the fusion index after 5 d culture in differentiation media (error = SD; * = $P < 0.05$ compared to untreated cellulate).

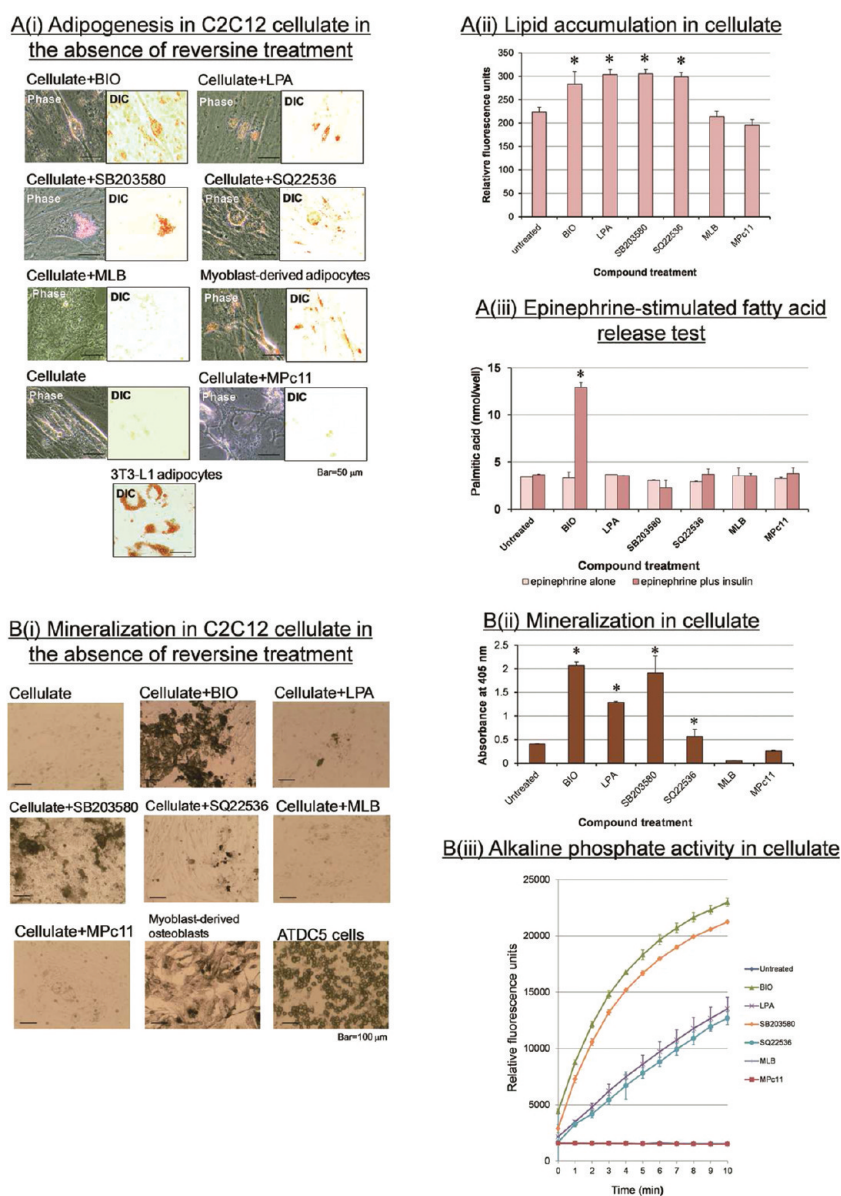


Figure 4. Analysis of adipogenesis and osteogenesis. (A) (i) Treatment of C2C12 muscle cellulate with $2.5 \mu\text{M}$ BIO, $10 \mu\text{M}$ SB203580, $300 \mu\text{M}$ SQ22536, or $30 \mu\text{M}$ LPA for 48 h, followed by treatment with adipogenic factors for 7 days, induced lipid deposition, which is a feature of adipogenic conversion. Lipid was visualized by oil Red O staining. Untreated C2C12 cellulate or treatment of C2C12 muscle cellulate with $50 \mu\text{M}$ MLB or $5 \mu\text{M}$ MPc11 for 48 h, followed by culture with adipogenic factors, did not show lipid deposition. C2C12 myoblasts treated with 250 nM reversine for 48 h and cultured in adipogenic media also accumulated lipid. Lipid accumulation in 3T3-L1 adipocytes is also shown for comparison. (ii) Lipid deposition could be measured by AdipoRed labeling. Treatment of C2C12 muscle cellulate with $2.5 \mu\text{M}$ BIO, $10 \mu\text{M}$ SB203580, $300 \mu\text{M}$ SQ22536, or $30 \mu\text{M}$ LPA for 48 h, followed by treatment with adipogenic factors, significantly increased lipid deposition. In contrast, untreated C2C12 cellulate or treatment of C2C12 muscle cellulate with $50 \mu\text{M}$ MLB or $5 \mu\text{M}$ MPc11 for 48 h, followed by culture with adipogenic factors, did not increase lipid deposition (error = SD; * = $P < 0.05$ compared to untreated cellulate). (iii) C2C12 cellulate treated with $2.5 \mu\text{M}$ BIO for 48 h, followed by treatment with adipogenic factors, showed insulin-sensitive free fatty acid release after epinephrine-stimulation (an adipocyte-specific function). In contrast, untreated C2C12 cellulate or treatment of C2C12 muscle cellulate with $10 \mu\text{M}$ SB203580, $300 \mu\text{M}$ SQ22536, $30 \mu\text{M}$ LPA, $50 \mu\text{M}$ MLB, or $5 \mu\text{M}$ MPc11 for 48 h, followed by culture with adipogenic factors, did not induce this adipocyte-specific function (error = SD; * = $P < 0.05$ compared to epinephrine alone; data are representative of three independent experiments). (B) (i) Treatment of C2C12 muscle cellulate with $2.5 \mu\text{M}$ BIO, $10 \mu\text{M}$ SB203580, $300 \mu\text{M}$ SQ22536, or $30 \mu\text{M}$ LPA for 48 h, followed by treatment with osteogenic factors induced mineralization, which is a feature of osteogenic conversion. Untreated cellulate or treatment of C2C12 muscle cellulate with $50 \mu\text{M}$ MLB or $5 \mu\text{M}$ MPc11 for 48 h, followed by culture with adipogenic factors, did not show mineralization. (ii) Treatment of C2C12 muscle cellulate with BIO, SB203580, SQ22536, or LPA for 48 h, followed by treatment with osteogenic factors, significantly increased mineralization. In contrast, untreated C2C12 muscle cellulate or treatment of C2C12 muscle cellulate with MLB or MPc11 for 48 h, followed by culture with osteogenic factors, did not increase mineralization (error = SD; * = $P < 0.05$ compared to untreated cellulate). (iii) Increased alkaline phosphatase activity is a feature of osteogenic conversion. Treatment of C2C12 muscle cellulate with BIO, SB203580, SQ22536, or LPA for 48 h, followed by treatment with osteogenic factors, significantly increased alkaline phosphatase activity. In contrast, untreated C2C12 cellulate or treatment of C2C12 muscle cellulate with MLB or MPc11 for 48 h, followed by culture with osteogenic factors, did not increase alkaline phosphatase activity. The assay values for untreated C2C12 muscle cellulate, MLB, and MPc11 were similar and cannot be separated on the graph.

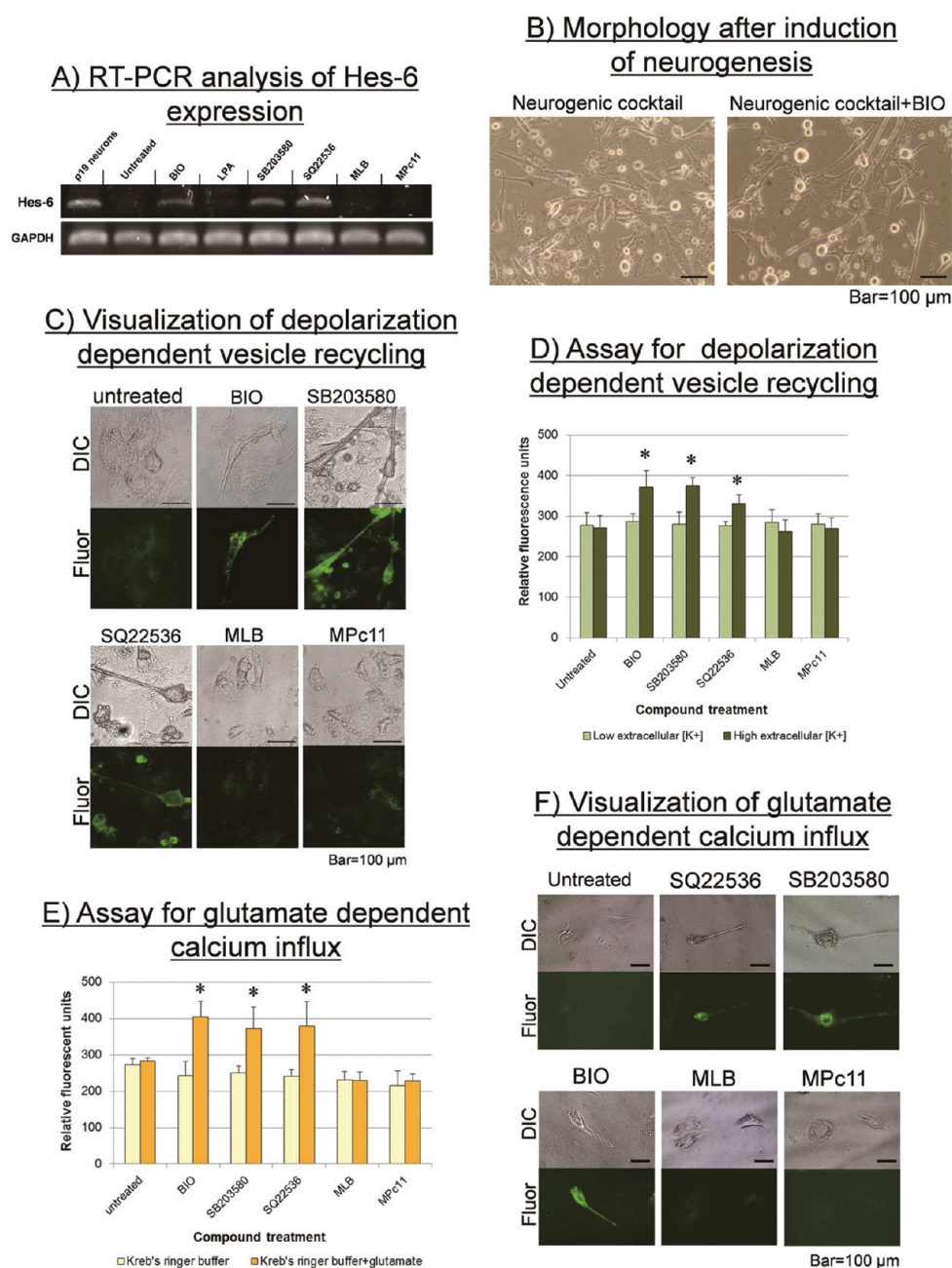


Figure 5. Analysis of neurogenesis. (A) Treatment of C2C12 muscle cellulate with 2.5 μM BIO, 10 μM SB203580, or 300 μM SQ22536 for 48 h, followed by treatment with 250 nM reversine for 48 h and culture in neurogenic media, induced expression of the neurogenic transcription factor, Hes-6. In contrast, treatment of C2C12 muscle cellulate with 30 μM LPA, 50 μM MLB, or 5 μM MPc11 for 48 h, followed by treatment with 250 nM reversine for 48 h and culture in neurogenic media, did not induce Hes-6 expression. (B) Treatment of the C2C12 muscle cellulate with BIO, followed by treatment with 250 nM reversine for 48 h and culture in neurogenic media, induced morphological changes consistent with neurogenesis. (C) Treatment of C2C12 muscle cellulate with BIO, SB203580, or SQ22536 for 48 h, followed by treatment with 250 nM reversine for 48 h and culture in neurogenic factors, conferred the ability to undergo depolarization-dependent vesicle recycling, which is a neuron-specific property. Vesicle recycling was visualized using the fluorescent probe, FM1-43. In contrast, treatment of C2C12 muscle cellulate with MLB or MPc11 for 48 h, followed by treatment with 250 nM reversine for 48 h and culture in neurogenic factors, did not confer depolarization-dependent vesicle recycling. (D) Treatment of C2C12 muscle cellulate with BIO, SB203580, or SQ22536 for 48 h, followed by treatment with 250 nM reversine for 48 h and culture in neurogenic factors, increased FM1-43 uptake after depolarization using high (100 mM) extracellular potassium. In contrast, treatment of C2C12 muscle cellulate with MLB or MPc11 for 48 h, followed by treatment with 250 nM reversine for 48 h and culture in neurogenic factors, did not confer depolarization-dependent increases in FM1-43 fluorescent signal (error = SD; * = $P < 0.05$ compared to low extracellular potassium). (E) Treatment of C2C12 muscle cellulate with BIO, SB203580, or SQ22536 for 48 h, followed by treatment with 250 nM reversine for 48 h and culture in neurogenic factors conferred the ability to undergo glutamate-dependent calcium influx, which is a neuron-specific property (error = SD; * = $P < 0.05$ compared to Krebs' ringer buffer treated group (minus glutamate)). (F) Glutamate-dependent calcium influx was visualized using the fluorescent probe, Fluo-3. Treatment of C2C12 muscle cellulate with BIO, SB203580, or SQ22536 for 48 h, followed by treatment with 250 nM reversine for 48 h and culture in neurogenic factors, produced cells that showed increased Fluo-3 signal after glutamate treatment. In contrast, treatment of C2C12 muscle cellulate with MLB or MPc11 for 48 h, followed by treatment with 250 nM reversine for 48 h and culture in neurogenic factors, did not produce cells that showed increased Fluo-3 signal.

in the cellulate, which are consistent with the onset of neurogenic conversion (Figure 5B).²⁹

Synaptic vesicle recycling is a property of nerve terminals and the fluorescent dye FM1-43 is used to label nerves undergoing synaptic vesicle recycling.³⁰ FM1-43 is internalized during synaptic vesicle recycling induced by potassium-dependent depolarization. This is an inherent property of neurons and is not observed in muscle.³¹ Treatment with BIO, SB203580, or SQ22536, followed by culture with reversine and neurogenic factors, induced depolarization-dependent vesicle recycling in the cellulate (Figure 5C). This was confirmed using a microplate reader-based assay (Figure 5D). Depolarization-dependent vesicle recycling achieved by p19 neurons is shown in Supplementary Figure 5 for comparison.

Glutamate is the major excitatory amino acid in the central nervous system, and glutamate-induced calcium influx is an intrinsic property of neurons.³¹ Intracellular calcium levels can be measured using the fluorescent indicator, Fluo-3.³¹ Cellulate treatment with BIO, SB203580, or SQ22536, followed by culture with reversine and neurogenic factors, induced glutamate-dependent calcium influx (Figure 5E,F).

BIO Treatment Produced Global Changes in Cellulate Gene Expression. Microarray analysis was employed to characterize cellulate dedifferentiation by small molecules. BIO was chosen for this study, and microarray analysis revealed that BIO-treated multipotent C2C12 muscle cellulate had a markedly different gene expression pattern compared to lineage-restricted C2C12 myoblasts (Figure 6A; full microarray

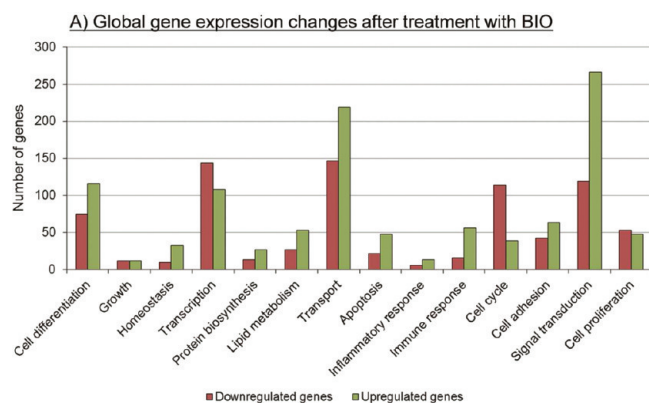


Figure 6. Microarray analysis showing global gene expression changes in 2.5 μM BIO-treated C2C12 cellulate (proliferating, multipotent cells) versus lineage restricted C2C12 myoblasts. The cellulate was treated with BIO for 48 h.

data deposited in the GEO database: accession number GSE34238). BIO-treated cellulate showed the largest changes in gene expression related to signal transduction, which is similar to myoblasts treated with the dedifferentiation-inducing small molecule, reversine.²⁹ The expression of genes linked to cellular transport processes, transcription, and cellular differentiation were also altered in the BIO-treated C2C12 cellulate. BIO treatment affected the expression of >200 genes linked to cell differentiation (listed in Supplementary Table 1).

BIO-treated C2C12 muscle cellulate is capable of proliferation (Figure 2B). Microarray analysis revealed that approximately 100 cell proliferation-related genes show altered expression (Figure 4A). Kyoto Encyclopedia of Genes and Genomes (KEGG) analysis of the p53 signaling pathway

showed that 9 out of 10 genes have reduced expression, including homologues of CHK2 cell cycle checkpoint and checkpoint kinase 1 (Supplementary Table 2). p53 signaling activates p21 to induce cell cycle arrest.³² Down-regulation of this pathway could provide a mechanism for the BIO-treated cellulate to escape cell cycle arrest and proliferate.

Microarray analysis was undertaken to further characterize neuronal cells derived from the BIO and reversine-treated cellulate. KEGG pathway analysis showed increased expression of genes linked to neuronal signaling compared to C2C12 myoblasts (Supplementary Table 3; full microarray data deposited in the GEO database: accession number GSE34238). In particular, subunits of the γ -aminobutyric acid (GABA) receptor are up-regulated. In addition, the majority of components of the mTOR and VEGF signaling are up-regulated (shown in Supplementary Tables 4 and 5); both of these pathways are important for mediating neurogenesis.^{33,34}

Dedifferentiated Cells Can Be Derived from Primary Muscle Culture Using BIO. Primary myotubes were obtained from 14-day-old BALB/c murine myoblasts. Myotubes were cellularized with 20 μM myoseverin for 48 h and treated with 2.5 μM BIO for 48 h. The cellulate proliferated after BIO treatment (as indicated by increased DNA synthesis) and dedifferentiated (Figure 7A,B). Subsequent treatment with adipogenic factors produced adipogenic cells (Figure 7C,D). Alternatively, treatment with osteogenic factors for 10 d produced osteogenic cells (Figure 7E,F). Cellulate treatment with 2.5 μM BIO for 48 h, followed by treatment with 250 nM reversine for 48 h and neurogenic factors for 7 d, produced cells with neuronal characteristics (Figure 7G,H).

In the animal kingdom, limb regeneration in urodele amphibians is a relatively dramatic example of tissue regeneration, involving muscle cellularization and cell cycle reentry.^{4,5} Our results suggest that multiple biochemical pathways can be manipulated to induce cellulate proliferation. We believe our results are significant, because we establish BIO, LPA, SQ22536, and SB203580 as dedifferentiation-inducing agents. In addition, the functional classification of these agents should be different from that of the known small molecule dedifferentiation agent, reversine, because BIO, LPA, SQ22536, and SB203580 also induce a proliferative response (it was previously shown that reversine requires cell cycle progression to be effective).³⁵

Previous studies of muscle cell dedifferentiation assessed lineage-specific gene expression or phenotypic markers, such as lipid accumulation during adipogenesis.²⁵ Our study attempted to monitor cell fate using more rigorous, functional assays, such as insulin-stimulated glucose uptake for assessing adipogenesis, mineralization for assessing osteogenesis, and glutamate-stimulated calcium influx for assessing neurogenesis. We believe that functional assays are preferable to the analysis of cell-type-specific markers, because acquisition of a cell-type-specific function is likely to require the expression of multiple cell markers, along with their appropriate functioning within the cell.

Pluripotency is defined as the ability of a cell population to differentiate into the three germ layers (endoderm, mesoderm, and ectoderm) and their differentiated derivatives.² In this study, we have shown that muscle cellulate treated with BIO, SB203580, or SQ22536, followed by reversine treatment, could differentiate into cells with neurogenic characteristics (Figure 5).

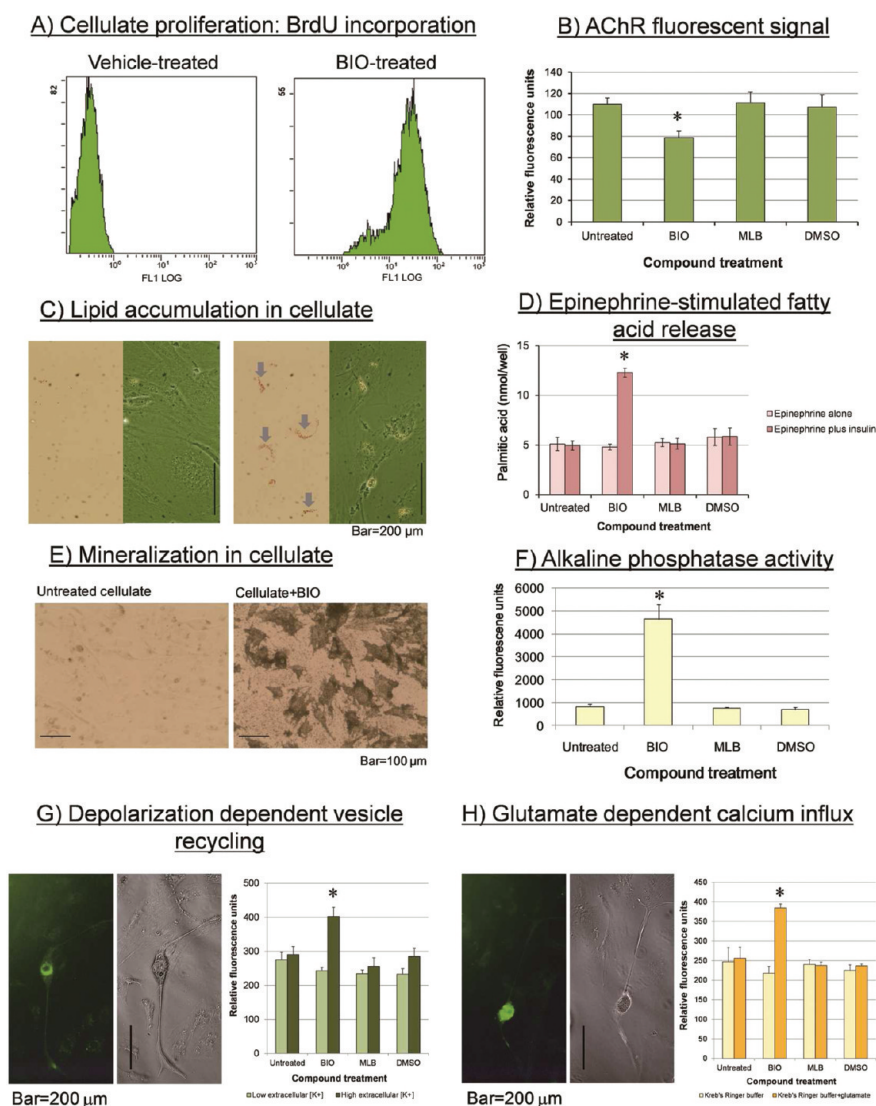


Figure 7. Analysis of cellulate derived from primary myotube cultures. (A) Cellulate treated with 2.5 μM BIO for 48 h showed induction of DNA synthesis, as shown by increased FITC-BrdU signal. Treatment of the C2C12 muscle cellulate with DMSO vehicle for 48 h did not increase DNA synthesis. (B) Fluorescent microplate reader assay for FITC-conjugated α -bungarotoxin labeling confirmed that treatment of the primary muscle cellulate with BIO enhanced dedifferentiation, as shown by reduced fluorescent signal. In contrast, treatment with 50 μM MLB for 48 h or DMSO failed to induce dedifferentiation (error = SD; * = $P < 0.05$ compared to untreated cellulate; data are representative of three independent experiments). (C) Treatment of the primary muscle cellulate with 2.5 μM BIO for 48 h, followed by treatment with adipogenic factors for 7 days, induced lipid deposition, which is a feature of adipogenic conversion. Lipid was visualized by oil Red O staining. Untreated primary cellulate or treatment of C2C12 muscle cellulate with 50 μM MLB or DMSO for 48 h, followed by culture with adipogenic factors, did not show lipid deposition. Blue arrows indicate areas of lipid staining. (D) Primary muscle cellulate treated with 2.5 μM BIO for 48 h, followed by treatment with adipogenic factors, showed insulin-sensitive free fatty acid release after epinephrine-stimulation (an adipocyte-specific function). In contrast, untreated C2C12 cellulate or treatment of C2C12 muscle cellulate with 50 μM MLB or DMSO for 48 h, followed by culture with adipogenic factors, did not possess this adipocyte-specific function (error = SD; * = $P < 0.05$ compared to epinephrine alone; data are representative of three independent experiments). (E) Treatment of the primary muscle cellulate with 2.5 μM BIO for 48 h, followed by treatment with osteogenic factors, significantly increased mineralization, as shown by alizarin red staining. Untreated primary cellulate or treatment of C2C12 muscle cellulate with 50 μM MLB or DMSO for 48 h, followed by culture with osteogenic factors, did not increase mineralization. (F) The BIO-treated cellulate also showed increased alkaline phosphatase activity, another feature of osteogenic conversion (error = SD; * = $P < 0.05$ for increased activity compared to untreated cellulate; data are representative of three independent experiments). (G) Treatment of the primary muscle cellulate with 2.5 μM BIO for 48 h, followed by treatment with 250 nM reversine for 48 h and neurogenic factors, produced cells capable of depolarization-dependent vesicle recycling, which is a neuron-specific property. Cells with characteristic neuronal morphology showed increased signal from the FM1-43 probe. In contrast, replacement of BIO treatment with 50 μM MLB or DMSO for 48 h failed to produce this effect (error = SD; * = $P < 0.05$ for increased FM1-43 signal compared to untreated cellulate; data are representative of three independent experiments). (H) Treatment of the primary muscle cellulate with 2.5 μM BIO for 48 h, followed by treatment with 250 nM reversine for 48 h and neurogenic factors, produced cells capable of glutamate-dependent calcium influx, which is a neuron-specific property. Cells with characteristic neuronal morphology showed increased signal from the Fluo-3 probe. In contrast, replacement of BIO treatment 50 μM MLB or DMSO for 48 h failed to induce glutamate-dependent calcium influx (error = SD; * = $P < 0.05$ for increased Fluo-3 signal compared to untreated cellulate; data are representative of three independent experiments).

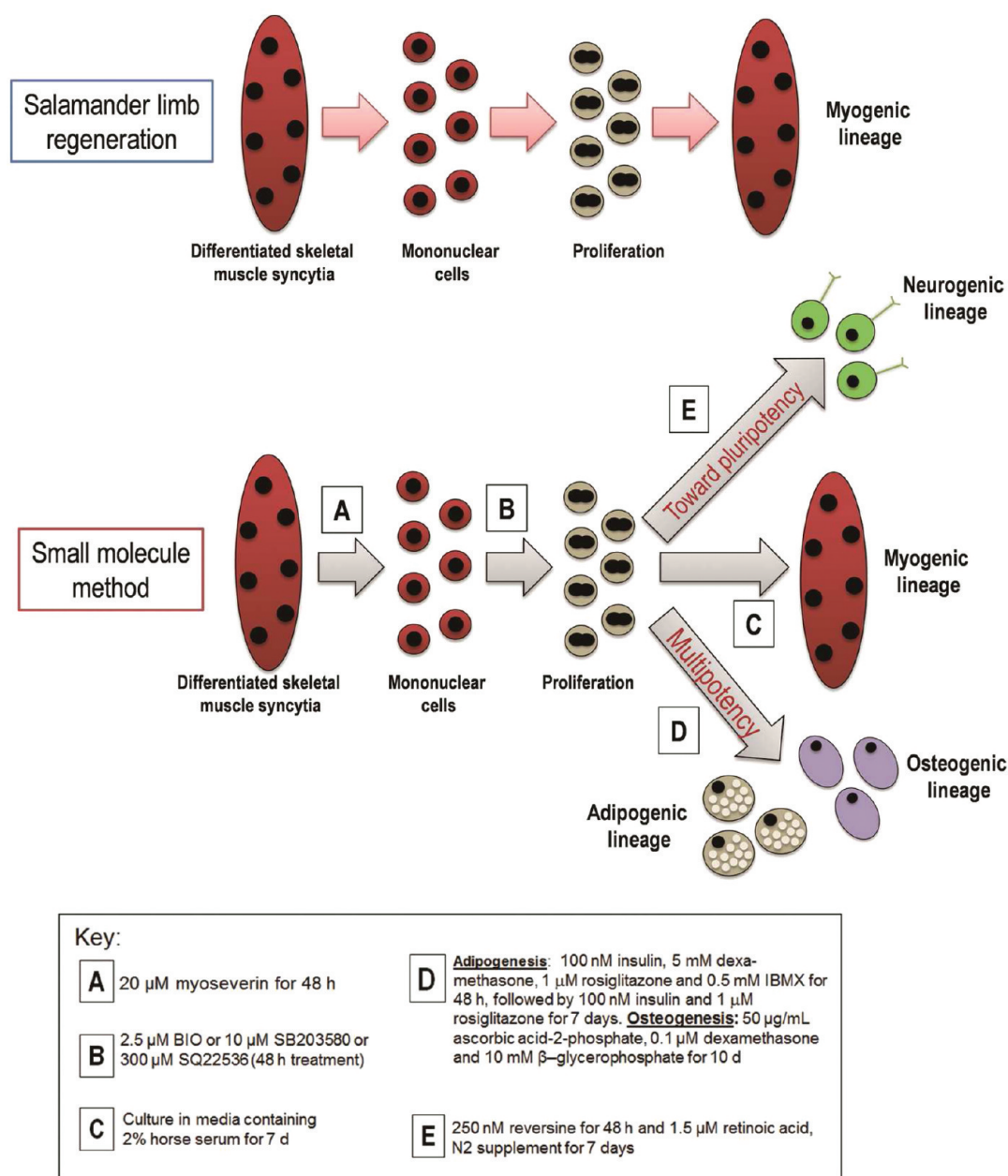


Figure 8. Schematic diagram of the small molecule method to obtain pluripotent cells from terminally differentiated skeletal muscle tissue. Recently published data suggest that in urodele amphibians, such as the salamander, muscle tissue dedifferentiates during limb regeneration and ultimately forms muscle tissue in the new limb (*i.e.*, unipotent cells).³⁶ The small molecule method described in this paper confers a greater degree of cellular plasticity to mammalian muscle tissue, producing dedifferentiation into cells that possess potential pluripotent characteristics, as shown by their conversion into cells displaying neurogenic properties. Please note that LPA is omitted from the scheme because LPA treatment could not induce the acquisition of neurogenic characteristics.

However, recent research indicates that during urodele amphibian limb regeneration dedifferentiated myotubes are lineage restricted and only form new muscle tissue.³⁶ In contrast, recent data from a fish model of appendage regeneration suggest that low level expression of pluripotency markers are linked to the regeneration mechanism, where blastema cells become “stalled” in an early, partially reprogrammed state, producing multipotent cells.³⁷ Moreover, mice with digit amputation and exogenous treatment with extracellular matrix molecules showed recruitment of multipotent cells to the injury site. The authors of this study speculated that the recruitment of multipotent cells to a site of injury that would not normally be populated by such cells, at least in such great numbers, could

promote a regenerative response.³⁸ A schematic of our own small molecule approach to derive multipotent cells from differentiated skeletal muscle tissue is shown in Figure 8.

Conclusion. Our small-molecule-based method for inducing dedifferentiation offers a number of areas for further study. For example, human muscle biopsies could be utilized to observe if patient-specific multipotent cells can be generated. Moreover, it may be interesting to attempt to transfer this method to mammalian models of wound healing. The small molecules used in this study (BIO, LPA, SB203580, and SQ22536) were shown to down-regulate p21 expression. The Murphy Roth Large mouse displays enhanced wound healing, which is also linked to reduced p21 expression.³⁹ Thus, these

small molecules could form the basis of a topical, medical application to enhance wound healing and reduce scarring. Off target effects are also an important consideration when using small molecules.⁴⁰ Thus, further study should focus on validating the target mechanisms of the small molecules used in this study. For example, this could be achieved by comparing the effects of alternative compounds or siRNA approaches that modulate the same biological targets as the small molecules used in this study. The adipogenic, osteogenic, and neurogenic cell types derived by small molecule treatment could also be characterized in more detail, for example, by assessing their function *in vivo*. Overall, we believe that the results of our study have interesting implications for the development of methods to enhance regeneration in mammals and suggest new approaches for deriving pluripotent stem cells from terminally differentiated mammalian tissues.

METHODS

A description of the following experimental methods can be found in the Supporting Information accompanying this manuscript: reagents, flow cytometry, MTT assay, labeling of acetylcholine receptors, fusion index, quantification and visualization of lipid accumulation, insulin-stimulated glucose uptake assay, alkaline phosphatase assay, alizarin red staining, quantification of mineralization, detection of synaptic vesicle recycling, detection of glutamate-dependent calcium influx, Western blotting, RT-PCR and primary myoblast culture.

ASSOCIATED CONTENT

Supporting Information

This material is available free of charge *via* the Internet at <http://pubs.acs.org>.

AUTHOR INFORMATION

Corresponding Author

*E-mail: darren@gist.ac.kr.

Author Contributions

[†]These authors contributed equally to this work.

Notes

The authors declare no competing financial interest.

ACKNOWLEDGMENTS

This research was supported by two grants from the National Research Foundation funded by the Korean government (MEST basic science research program (NRF-2010-0006002) to D.W. and MEST basic science research program (NRF-2009-0067894) to D.J.). We also acknowledge the Bioimaging Research Center, Gwangju Institute of Science and Technology.

REFERENCES

- (1) Grafi, G. (2009) The complexity of cellular dedifferentiation: implications for regenerative medicine. *Trends Biotechnol.* 27, 329–332.
- (2) Lyssiotis, C. A., Lairson, L. L., Boitano, A. E., Wurdak, H., Zhu, S., and Schultz, P. G. (2011) Chemical control of stem cell fate and developmental potential. *Angew. Chem., Int. Ed.* 50, 200–242.
- (3) Xu, Y., Shi, Y., and Ding, S. (2008) A chemical approach to stem-cell biology and regenerative medicine. *Nature* 453, 338–344.
- (4) Tweedell, K. S. (2010) The urodele limb regeneration blastema: the cell potential. *TheScientificWorldJournal* 10, 954–971.
- (5) Brockes, J. P., and Kumar, A. (2002) Plasticity and reprogramming of differentiated cells in amphibian regeneration. *Nat. Rev. Mol. Cell Biol.* 3, 566–574.
- (6) Brockes, J. P., and Kumar, A. (2008) Comparative aspects of animal regeneration. *Annu. Rev. Cell Dev. Biol.* 24, 525–549.
- (7) Endo, T. (2007) Stem cells and plasticity of skeletal muscle cell differentiation: potential application to cell therapy for degenerative muscular diseases. *Regener. Med.* 2, 243–256.
- (8) Odelberg, S. J., Kollhoff, A., and Keating, M. T. (2000) Dedifferentiation of mammalian myotubes induced by *msx1*. *Cell* 103, 1099–1109.
- (9) Jung, D. W., and Williams, D. R. (2011) Novel chemically defined approach to produce multipotent cells from terminally differentiated tissue syncytia. *ACS Chem. Biol.* 6, 553–562.
- (10) Pajcini, K. V., Corbel, S. Y., Sage, J., Pomerantz, J. H., and Blau, H. M. (2010) Transient inactivation of Rb and ARF yields regenerative cells from postmitotic mammalian muscle. *Cell Stem Cell* 7, 198–213.
- (11) Bruna, S., Dapas, B., Farra, R., Grassi, M., Pozzato, G., Giansante, C., Fiotti, N., and Grassi, G. (2011) Improving siRNA bio-distribution and minimizing side effects. *Curr. Drug Metab.* 12, 11–23.
- (12) Fedorov, Y., Anderson, E. M., Birmingham, A., Reynolds, A., Karpilov, J., Robinson, K., Leake, D., Marshall, W. S., and Khvorova, A. (2006) Off-target effects by siRNA can induce toxic phenotype. *RNA* 12, 1188–1196.
- (13) Perez, O. D., Chang, Y. T., Rosania, G., Sutherlin, D., and Schultz, P. G. (2002) Inhibition and reversal of myogenic differentiation by purine-based microtubule assembly inhibitors. *Chem. Biol.* 9, 475–483.
- (14) Duckmanton, A., Kumar, A., Chang, Y. T., and Brockes, J. P. (2005) A single-cell analysis of myogenic dedifferentiation induced by small molecules. *Chem. Biol.* 12, 1117–1126.
- (15) Rhim, J. H., Jang, I. S., Song, K. Y., Ha, M. K., Cho, S. C., Yeo, E. J., and Park, S. C. (2008) Lysophosphatidic acid and adenyllyl cyclase inhibitor increase proliferation of senescent human diploid fibroblasts by inhibiting adenosine monophosphate-activated protein kinase. *Rejuvenation Res.* 11, 781–792.
- (16) Pajalunga, D., Mazzola, A., Salzano, A. M., Biferi, M. G., De Luca, G., and Crescenzi, M. (2007) Critical requirement for cell cycle inhibitors in sustaining nonproliferative states. *J. Cell Biol.* 176, 807–818.
- (17) de Carne Trecesson, S., Guillemin, Y., Belanger, A., Bernard, A. C., Preisser, L., Ravon, E., Gamelin, E., Juin, P., Barre, B., and Coqueret, O. (2011) Escape from p21-mediated oncogene-induced senescence leads to cell dedifferentiation and dependence on anti-apoptotic Bcl-xL and MCL1 proteins. *J. Biol. Chem.* 286, 12825–12838.
- (18) Cuenda, A., and Rousseau, S. (2007) p38 MAP-kinases pathway regulation, function and role in human diseases. *Biochim. Biophys. Acta* 1773, 1358–1375.
- (19) Tseng, A. S., Engel, F. B., and Keating, M. T. (2006) The GSK-3 inhibitor BIO promotes proliferation in mammalian cardiomyocytes. *Chem. Biol.* 13, 957–963.
- (20) Williams, D., Jung, D. W., Khersonsky, S. M., Heidary, N., Chang, Y. T., and Orlow, S. J. (2004) Identification of compounds that bind mitochondrial F1F0 ATPase by screening a triazine library for correction of albinism. *Chem. Biol.* 11, 1251–1259.
- (21) Kim, S. H., Choi, M., Lee, Y., Kim, Y. O., Ahn, D. S., Kim, Y. H., Kang, E. S., Lee, E. J., Jung, M., Cho, J. W., Williams, D. R., and Lee, H. C. (2010) Natural therapeutic magnesium lithospermate B potently protects the endothelium from hyperglycaemia-induced dysfunction. *Cardiovasc. Res.* 87, 713–722.
- (22) Barbero, A., Benelli, R., Minghelli, S., Tosetti, F., Dorcaratto, A., Ponzetto, C., Wernig, A., Cullen, M. J., Albin, A., and Noonan, D. M. (2001) Growth factor supplemented matrigel improves ectopic skeletal muscle formation--a cell therapy approach. *J. Cell Physiol.* 186, 183–192.
- (23) Myers, T. K., Andreuzza, S. E., and Franklin, D. S. (2004) p18INK4c and p27KIP1 are required for cell cycle arrest of differentiated myotubes. *Exp. Cell Res.* 300, 365–378.
- (24) Jung, D. W., Ha, H. H., Zheng, X., Chang, Y. T., and Williams, D. R. (2011) Novel use of fluorescent glucose analogues to identify a new class of triazine-based insulin mimetics possessing useful secondary effects. *Mol. Biosyst.* 7, 346–358.
- (25) Nishide, M., Yoshikawa, Y., Yoshikawa, E. U., Matsumoto, K., Sakurai, H., and Kajiwara, N. M. (2008) Insulinomimetic Zn(II)

complexes as evaluated by both glucose-uptake activity and inhibition of free fatty acids release in isolated rat adipocytes. *Chem. Pharm. Bull. (Tokyo)* 56, 1181–1183.

(26) Hall, B. K., and Miyake, T. (1992) The membranous skeleton: the role of cell condensations in vertebrate skeletogenesis. *Anat. Embryol. (Berlin)* 186, 107–124.

(27) Anderson, H. C. (1969) Vesicles associated with calcification in the matrix of epiphyseal cartilage. *J. Cell Biol.* 41, 59–72.

(28) Gregory, C. A., Gunn, W. G., Peister, A., and Prockop, D. J. (2004) An Alizarin red-based assay of mineralization by adherent cells in culture: comparison with cetylpyridinium chloride extraction. *Anal. Biochem.* 329, 77–84.

(29) Lee, E. K., Bae, G. U., You, J. S., Lee, J. C., Jeon, Y. J., Park, J. W., Park, J. H., Ahn, S. H., Kim, Y. K., Choi, W. S., Kang, J. S., Han, G., and Han, J. W. (2009) Reversine increases the plasticity of lineage-committed cells toward neuroectodermal lineage. *J. Biol. Chem.* 284, 2891–2901.

(30) Betz, W. J., and Bewick, G. S. (1992) Optical analysis of synaptic vesicle recycling at the frog neuromuscular junction. *Science* 255, 200–203.

(31) Watanabe, Y., Kameoka, S., Gopalakrishnan, V., Aldape, K. D., Pan, Z. Z., Lang, F. F., and Majumder, S. (2004) Conversion of myoblasts to physiologically active neuronal phenotype. *Genes Dev.* 18, 889–900.

(32) He, G., Siddik, Z. H., Huang, Z., Wang, R., Koomen, J., Kobayashi, R., Khokhar, A. R., and Kuang, J. (2005) Induction of p21 by p53 following DNA damage inhibits both Cdk4 and Cdk2 activities. *Oncogene* 24, 2929–2943.

(33) Jin, K., Zhu, Y., Sun, Y., Mao, X. O., Xie, L., and Greenberg, D. A. (2002) Vascular endothelial growth factor (VEGF) stimulates neurogenesis in vitro and in vivo. *Proc. Natl. Acad. Sci. U.S.A.* 99, 11946–11950.

(34) Han, J., Wang, B., Xiao, Z., Gao, Y., Zhao, Y., Zhang, J., Chen, B., Wang, X., and Dai, J. (2008) Mammalian target of rapamycin (mTOR) is involved in the neuronal differentiation of neural progenitors induced by insulin. *Mol. Cell. Neurosci.* 39, 118–124.

(35) Chen, S., Takahashi, S., Zhang, Q., Xiong, W., Zhu, S., Peters, E. C., Ding, S., and Schultz, P. G. (2007) Reversine increases the plasticity of lineage-committed mammalian cells. *Proc. Natl. Acad. Sci. U.S.A.* 104, 10482–10487.

(36) Kragl, M., Knapp, D., Nacu, E., Khattak, S., Maden, M., Epperlein, H. H., and Tanaka, E. M. (2009) Cells keep a memory of their tissue origin during axolotl limb regeneration. *Nature* 460, 60–65.

(37) Christen, B., Robles, V., Raya, M., Paramonov, I., and Belmonte, J. C. (2010) Regeneration and reprogramming compared. *BMC Biol.* 8, 5.

(38) Agrawal, V., Johnson, S. A., Reing, J., Zhang, L., Tottey, S., Wang, G., Hirschi, K. K., Braunhut, S., Gudas, L. J., and Badyrak, S. F. (2010) Epimorphic regeneration approach to tissue replacement in adult mammals. *Proc. Natl. Acad. Sci. U.S.A.* 107, 3351–3355.

(39) Bedelbaeva, K., Snyder, A., Gourevitch, D., Clark, L., Zhang, X. M., Leferovich, J., Cheverud, J. M., Lieberman, P., and Heber-Katz, E. (2010) Lack of p21 expression links cell cycle control and appendage regeneration in mice. *Proc. Natl. Acad. Sci. U.S.A.* 107, 5845–5850.

(40) Weiss, W. A., Taylor, S. S., and Shokat, K. M. (2007) Recognizing and exploiting differences between RNAi and small-molecule inhibitors. *Nat. Chem. Biol.* 3, 739–744.